C.P. No. 1005

C.P. No. 1005

MINISTRY OF TECHNOLOGY

AERONAUTICAL RESEARCH COUNCIL

CURRENT PAPERS

The Calculation of the Pressure Distribution on a Thick Cambered Aerofoil at Subsonic Speeds Including the Effects of the Boundary Layer

By

B. J. Powell

LONDON: HER MAJESTY'S STATIONERY OFFICE

SIX SHILLINGS NET

C.P. No.1005*

June, 1967

The Calculation of the Pressure Distribution on a Thick Cambered Aerofoil at Subsonic Speeds including the Effects of the Boundary Layer

- By -
B. J. Powell

SUMMARY

This paper describes a method for calculating the pressure distribution on the surface of a two-dimensional aerofoil of arbitrary shape in subsonic flow, taking into account the presence of a boundary layer on the surface of the aerofoil. The effect of the boundary layer is accounted for by considering the inviscid flow over a displacement surface made up of the aerofoil section shape, boundary layer displacement thickness and the wake. A simple model of the wake is introduced, and it is shown that provided certain simple conditions are satisfied in the region near the aerofoil trailing edge, the pressure distribution predicted is not unduly sensitive to the detailed development of the wake. The method has been developed using techniques which make it very suitable for computation on a digital computer. Calculations have been made of the pressure distribution on a RAE 101 aerofoil section at incidence for which measured boundary layer data were available, and also in the case of a heavily cambered aerofoil at incidence using theoretically predicted boundary layer characteristics. The comparison between the experimental and predicted pressure distributions shows good agreement in both cases.

List /

---

*Replaces NPL Aero Report 1238 - A.R.C.29 300

List of Contents

Notation/

Notation

x, z	non-dimensional co-ordinates measured along and normal to the chord-line of the aerofoil.
z_t, z_s	thickness and camber ordinates of the aerofoil section.
Z_t, Z_s	thickness and camber ordinates of the displacement surface.
z^*	thickness ordinate of the residual aerofoil, see Section 3.1.
δ_U^*, δ_L^*	boundary layer displacement thicknesses on the upper and lower surfaces of the aerofoil.
δ_w^*	total displacement thickness of the wake.
d^*	$\frac{1}{2}$ x total displacement thickness at the trailing edge of the aerofoil.
σ	$\left(\frac{dZ_t}{dx}\right)_{T.E.}$ see Section 2.5.
α	aerofoil incidence.
$\Delta\alpha$	change of incidence produced by differential boundary layer thickness on the upper and lower surfaces of the aerofoil.
α^*	incidence of the displacement surface.
ρ	leading edge radius of the aerofoil.
ρ^*	leading edge radius of the displacement surface.
C_p	pressure coefficient on the aerofoil surface.
M_o	free-stream Mach number.
$q(x), \gamma(x)$	strengths of the source and vortex distributions to make the displacement surface a streamline.
$S^{(n)}(x)$ n=1,2,3,4,5.	see Section 2.2 and Refs. 4 and 5.
$s_{\mu\nu}^{(n)}$ n=1,2,3,4,5.	see Section 3.1 and Refs. 4 and 5.
$S^{(n)*}(x)$	values of $S^{(n)}(x)$ evaluated for the residual aerofoil.
V	local velocity on the displacement surface.
V_o	free-stream velocity.
θ, H	momentum thickness and form parameter of the boundary layer.
C_L, C_D	lift and drag coefficients.
N	number of reference points taken along the chord.

X/

X	distance downstream of the trailing edge at which the wake displacement thickness is assumed to become constant.
β, B	compressibility factors.
$F(x), G(x)$	functions used to define the thickness distribution of the displacement surface.
P, Q	coefficients used to define the wake.
$\phi_1 \ldots \phi_4$	functions used in the calculation of $S^{(1)}(x)$.
$\chi_1 \ldots \chi_2$	functions used in the calculation of $S^{(2)}(x)$.
$\psi_1 \ldots \psi_5$	functions used in the calculation of $S^{(3)}(x)$.

suffices:

TE	value at the trailing edge of the aerofoil.
U, L	upper and lower surfaces of the aerofoil.
∞	value at large distance downstream of the aerofoil.

---

1. Introduction

The pressure distribution on the surface of an aerofoil in inviscid flow is determined by the aerofoil geometry, i.e., the thickness distribution, the shape of the camber line and the incidence. The circulation about the aerofoil and consequently the lift developed are determined primarily by the camber and incidence.

In the case of a symmetric aerofoil at zero incidence the circulation is zero, and the pressure distribution is dependent only on the thickness distribution. This is to a large extent a local problem in the sense that the pressure at a point on the aerofoil surface is determined almost entirely by the shape of the surface in the region of that point, and consequently any small alteration in the shape, i.e., the thickness distribution, will primarily affect the pressure in the region of the change, the pressure over the rest of the aerofoil being relatively unaffected. The presence of a boundary layer on the surface of the aerofoil will produce a distortion of the streamlines close to the surface equivalent to a change in the thickness distribution. Thus at zero incidence the effect of the boundary layer at any point is expected to depend mainly on the thickness of the boundary layer near that point, and significant changes in the pressure should occur only when the boundary layer thickness is significant, i.e. over the rearmost part of the aerofoil. Fig. 1 shows a comparison between the calculated inviscid pressure distribution and the measured (viscous) one on a 10% thick symmetric aerofoil at zero incidence. It will be observed that there is no significant difference between the two results except over the last few percent of the aerofoil chord, as expected.

In the general case of the flow about a thick aerofoil (symmetric or cambered) at incidence, the pressure distribution over the whole of the aerofoil is very dependent on the circulation which is itself dependent on the incidence and the growth of the boundary layer, particularly near the trailing edge. Thus the boundary layer characteristics near the trailing edge no longer just affect the pressure in that region, but by altering the circulation, change the pressure distribution significantly over the whole aerofoil. In Fig. 2 a comparison is presented which shows the measured pressure distribution and the theoretically predicted inviscid pressure distribution at the same incidence. The comparison indicates the drastic change in the pressure distribution due to viscous effects, the considerable loss of lift, and the necessity of a theory which will adequately account for the presence of the boundary layer.

Previous authors, Preston (Ref. 1) and Spence and Beasley (Ref. 2) have tackled the problem of predicting the reduction in circulation due to viscous effects and the resulting loss of lift. The purpose of the present report is to develop a method to deal with the more general problem of predicting the detailed pressure distribution over the surface of the aerofoil when the boundary layer characteristics are known.

The complete problem of calculating the pressure distribution on an aerofoil section in viscous flow can be broken down into two distinct problems for those cases where the effects of viscosity are confined to a thin layer adjacent to the surface of the aerofoil, i.e., the boundary layer. In such cases the flow outside the boundary layer is essentially potential flow, and the two complementary problems can be stated as follows:

(i) the calculation of the boundary layer characteristics over the surface of the aerofoil when the pressure distribution on the aerofoil is known;

(ii)/

(ii) the calculation of the pressure distribution on the aerofoil when the boundary layer characteristics, in particular the displacement thickness, are known.

This paper is concerned with the second of these problems. For methods of dealing with the first problem, the reader should consult Ref. 3. The calculation of the pressure distribution on an aerofoil of arbitrary shape ab initio, must involve both problems. It is envisaged that the calculation would take the form of an iteration between these two separate calculations, starting from some convenient initial approximation such as the inviscid pressure distribution.

If the boundary layer is thin, then the streamlines in the viscous flow just outside of the boundary layer are displaced relative to the corresponding streamlines in the inviscid flow, by an amount equal to the local boundary layer displacement thickness. The flow outside the boundary layer, which is essentially potential flow, is therefore very similar to the potential flow about a "displacement surface" formed by adding the boundary layer displacement thicknesses on each of the aerofoil surfaces to the basic aerofoil shape. Downstream of the trailing edge of the aerofoil the streamlines are displaced by an amount approximately equal to the displacement thickness of the wake; thus the displacement surface must be extended downstream in this manner. The displacement surface, unlike the basic aerofoil section which is closed at the trailing edge, is of infinite extent. However, only that part of the displacement surface which extends over the aerofoil chord is capable of sustaining a significant difference in pressure between its upper and lower surfaces. It has been shown that the potential flow over the displacement surface gives rise to a streamline pattern outside the boundary layer almost identical with that of the viscous flow about the aerofoil; in addition there must exist a surface such that the inviscid pressure distribution on this surface is the same as the viscous pressure distribution on the basic aerofoil. The hypothesis is made that this surface and the displacement surface defined above are for all practical purposes identical. The problem of calculating the viscous flow about an aerofoil therefore becomes the problem of calculating the inviscid flow about a surface of infinite extent, the displacement surface referred to above.

For consistency in terminology the terms "thickness distribution" and "camber line" will be retained with reference to the displacement surface. The thickness distribution is defined as the semi-height between the upper and lower surfaces, the camber line as the mean line between the two surfaces. The velocity field about the displacement surface will be simulated by distributions of sources and vortices, providing the symmetric and asymmetric components of the flow respectively, which make the displacement surface a streamline of the flow. The value of the circulation is fixed by the criterion, based on experimental evidence, that the ratio of the velocities on the upper and lower surfaces at the trailing edge is unity. This criterion replaces the Kutta condition which establishes the circulation in the case of an aerofoil with a sharp trailing edge, by positioning the rear stagnation point at the trailing edge.

2. Basic Method

2.1 Displacement surface

The displacement surface over the aerofoil chord has been defined as the surface generated when the boundary layer displacement thickness on the upper and lower surfaces of the aerofoil is added to the basic aerofoil section (Fig. 3). These increments should strictly be added normal to the aerofoil surface. In practice it is more convenient to add them normal to the chord line, the error introduced being small and in most cases inside the accuracy with which the displacement thickness distribution, measured or calculated, will be known. Thus the upper and lower surfaces are given by

$$Z_U = z_U + \delta_U^* \quad ; \quad Z_L = z_L - \delta_L^* \, . \qquad \ldots (1)$$

and the thickness distribution of the displacement surface is related to that of the basic aerofoil by

$$\begin{aligned} Z_t &= z_t + \tfrac{1}{2}(\delta_U^* + \delta_L^*) \qquad 0 \leqslant x \leqslant 1 \\ Z_t &= \tfrac{1}{2}\,\delta_w^* \qquad\qquad\qquad\quad x > 1 \end{aligned} \qquad \ldots (2)$$

The camber line has been defined as the mean line between the upper and lower displacement surfaces, for convenience taken normal to the chord line of the basic aerofoil. In general, the ordinate of the mean line at the trailing edge will not be zero (Fig. 3); thus the effect of the boundary layer will be to modify the camber line and to induce a change of incidence $\Delta\alpha$. The camber ordinates for the displacement surface are given by

$$Z_s = z_s + \tfrac{1}{2}(\delta_U^* - \delta_L^*) + x.\tan\Delta\alpha \qquad 0 \leqslant x \leqslant 1 \qquad \ldots (3)$$

$$\text{where} \quad \tan\Delta\alpha = -\tfrac{1}{2}(\delta_U^* - \delta_L^*)_{TE}$$

Thus the problem of calculating the pressure distribution about an aerofoil defined by (z_t, z_s) at incidence α with a boundary layer, becomes the problem of calculating the potential flow about the surface defined by (Z_t, Z_s) at incidence $\alpha^*(= \alpha + \Delta\alpha)$.

2.2 Symmetric flow about the displacement surface

The symmetric component of the flow is represented by a source distribution of strength $q(x)$ which generates a stream-surface having the same thickness distribution as the displacement surface. The required source strength can be related approximately to the local slope of the thickness distribution (Ref. 4),

$$q(x) = 2\,V_0 \frac{dZ_t}{dx} \qquad x > 0 \qquad \ldots (4)$$

and/

and the velocity distribution $V(x)$ evaluated on the surface, due to this source distribution, is given to a good approximation by

$$\left(\frac{V(x)}{V_0}\right)^2 = \frac{1}{1 + \left(\frac{dZ_t}{dx}\right)^2} \left[1 + \frac{1}{\pi} \int_0^\infty \frac{dZ_t}{dy} \frac{dy}{x - y}\right]^2 \quad \ldots (5)$$

Using the notation of Ref. 4, but defining $S^{(1)}(x)$ by

$$S^{(1)}(x) = \frac{1}{\pi} \int_0^\infty \frac{dZ_t}{dy} \frac{dy}{x - y} \quad \ldots (6)$$

and

$$S^{(2)}(x) = \frac{dZ_t}{dx} , \quad \ldots (7)$$

equation (5) becomes

$$\left(\frac{V(x)}{V_0}\right)^2 = \frac{[1 + S^{(1)}]^2}{1 + (S^{(2)})^2} \quad \ldots (8)$$

2.3 Asymmetric flow about the displacement surface

The asymmetric component of the flow is represented by a distribution of vortices along the mean line whose strength $\gamma(x)$ is related to the slope of the camber line, and which takes account of the fact that the velocity increments are to be evaluated on the displacement surface and not on the camber line itself. The contribution of the vorticity in the wake to the circulation about the aerofoil is negligible, and the assumption is made that the vorticity in the wake is zero. Hence, with this assumption, the vorticity distribution is contained within the chord of the aerofoil. The problem thus becomes one of finding the strength of the vorticity $\gamma(x)$ in terms of the shape of the camber line and the thickness distribution of the displacement surface. If the displacement surface were to be closed at the trailing edge then the problem would be identical to that for a conventional aerofoil in inviscid flow.

With the notation of Ref. 5, the velocity distribution about the displacement surface due to the combined effects of the source distribution $q(x)$ and the vortex distribution $\gamma(x)$ is given by

$$\left(\frac{V}{V_0}\right)^2 = \frac{\left[\cos\alpha^* \left(1 + S^{(1)} \pm S^{(4)}\right) \pm \sin\alpha^* \left(1 + S^{(3)}\right) \sqrt{\frac{1 - x}{x}}\right]^2}{1 + \left(S^{(2)} \pm S^{(5)}\right)^2} \quad \ldots (9)$$

and the pressure coefficient in incompressible flow is given by

$$C_p = 1 - \left(\frac{V}{V_0}\right)^2$$

where/

where $S^{(1)}(x)$ and $S^{(2)}(x)$ are defined by equations (6) and (7) respectively, and the definition of $S^{(3)}(x)$ is extended in a very simple manner to account for the fact that the displacement surface does not close at the trailing edge. $S^{(3)}(x)$, $S^{(4)}(x)$ and $S^{(5)}(x)$ are thus defined as follows:

$$S^{(3)}(x) = \frac{1}{\pi}\int_0^{\infty}\left[\frac{dZ_t}{dy} - \frac{Z_t}{2y(1-y)}\right]\frac{dy}{x-y} \qquad \ldots (10)$$

$$S^{(4)}(x) = \frac{1}{\pi}\sqrt{\frac{1-x}{x}}\int_0^{1}\frac{dZ_s}{dy}\sqrt{\frac{y}{1-y}}\frac{dy}{x-y} \qquad \ldots (11)$$

$$S^{(5)}(x) = \frac{dZ_s}{dx} \qquad \ldots (12)$$

The alternative signs in equation (9) refer to the upper and lower surfaces respectively.

If the boundary layer displacement thickness on the aerofoil and in the wake are known, then the functions $S^{(1)}(x)$ ..... $S^{(5)}(x)$ can be evaluated to give the velocity distribution over the displacement surface and hence the pressure distribution over the aerofoil with boundary layer.

2.4 Circulation about the aerofoil and conditions at the trailing edge

The value of the circulation is established by means of the criterion that the ratio between the velocities at the edge of the boundary layers on the upper and lower surfaces of the aerofoil, evaluated at the trailing edge, is unity. By virtue of the hypothesis made in Section 1, this becomes equivalent to the condition that the pressure on the displacement surface at the trailing edge is equal on the upper and lower surfaces. This requires that the vortex distribution must be chosen so that $\gamma(1) = 0$, and hence $S^{(4)}(1) = 0$. The streamlines outside the boundary layer are continuous and have continuity of slope even though the aerofoil has discontinuous slope at the trailing edge. Since the pressure on the aerofoil surface in the presence of a boundary layer is approximately equal to the pressure along the streamline just outside the boundary layer, there cannot be a stagnation point at the trailing edge as this would imply the existence of a discontinuity in slope of the streamline. The hypothesis that the displacement surface is such that the pressure distribution on it in inviscid flow is the same as the pressure distribution on the aerofoil in the viscous flow requires that there is no discontinuity in slope of the displacement surface at the trailing edge, and hence no stagnation point nor infinite velocity.

2.5 Displacement thickness of the wake

No satisfactory method exists at present for the prediction of the way in which the displacement thickness of the wake develops immediately downstream of the trailing edge. From momentum considerations etc., at large distances downstream of the trailing edge (i.e. as $x \to \infty$) we have $\theta_\infty = \frac{1}{2}C_D$ and $H_\infty = 1$. Thus the displacement thickness of the wake has a value of

$\frac{1}{2}C_D$/

$\frac{1}{2}C_D$ as $x \to \infty$. This, in conjunction with the constraints mentioned in Section 2.4, requires that the displacement thickness of the wake satisfies the conditions:

(i) $Z_t = d^*$ when $x = 1$, where $d^* = \frac{1}{2}(\delta_U^* + \delta_L^*)_{TE}$

(ii) dZ_t/dx is continuous at $x = 1$,

(iii) $Z_t \to C_D/4$ as $x \to \infty$.

A simple model of the wake is proposed which satisfies conditions (i) and (ii) at the trailing edge and has a displacement thickness which is assumed to reach the value $\frac{1}{2}C_D$ at some finite distance X downstream of the trailing edge and remain constant after that point. Using this model the wake thickness distribution can be approximated to by the function

$$Z_t = d^* + \sigma(x - 1) + P(x - 1)^2 + Q(x - 1)^3 \quad , \quad 1 \leq x \leq 1 + X$$
$$Z_t = C_D/4 \quad , \quad x > 1 + X \; . \qquad \ldots (13)$$

where

$$P = \frac{3C_D - 12d^* - 8\sigma X}{4X^2}$$

$$Q = \frac{-C_D + 4d^* + 2\sigma X}{2X^3}$$

It is shown in Appendix 2 that provided the continuity of the displacement surface and its slope are preserved at the trailing edge, the pressure on the aerofoil surface, even at the trailing edge, is not particularly sensitive to the detailed shape of the wake downstream of the trailing edge (e.g. to the value of X). For practical calculations a value of X in the range 0.2 to 0.3 should be satisfactory.

3. Numerical Method

3.1 Basic problem

The calculation of the velocity distribution on the displacement surface, and hence the pressure distribution on the aerofoil surface, requires the computation of the functions $S^{(1)}(x)$, $S^{(2)}(x)$, $S^{(3)}(x)$, $S^{(4)}(x)$, and $S^{(5)}(x)$ for the thickness and camber distributions of the displacement surface defined in equations (2), (3) and (13).

The functions $S^{(4)}(x)$ and $S^{(5)}(x)$ which depend on the camber ordinates can be computed by the numerical method developed by Weber (Ref. 5), i.e.,

$S^{(4)}(x)/$

$$S^{(4)}(x_\nu) = \sum_{\mu=1}^{N-1} s^{(4)}_{\mu\nu} Z_{s\mu} \qquad \ldots (14)$$

$$S^{(5)}(x_\nu) = \sum_{\mu=1}^{N-1} s^{(5)}_{\mu\nu} Z_{s\mu} \qquad \ldots (15)$$

where $x_\nu = \frac{1}{2}\left(1 + \cos \frac{\nu\pi}{N}\right)$. $\qquad \nu = 1,2,3.....N-1$.

and $s^{(n)}_{\mu\nu}$ are influence coefficients independent of the camber ordinates.

The method of Ref. 4 for the calculation of the functions $S^{(n)}(x)$, n=1,2,3, is designed to deal only with closed aerofoil thickness distributions and cannot be used in the present calculation.

It is convenient to subdivide the thickness distribution of the displacement surface over the aerofoil chord into three parts as shown in Fig. 3B.

$$Z_t = z^* + d^* F(x) - \sigma\, G(x) \qquad 0 \leqslant x \leqslant 1 \qquad \ldots (16)$$

where $F(x) = x^2(3-2x)$; $G(x) = x^2(1-x)$

Defined in this way, z^* which is referred to as the "residual thickness", satisfies the conditions,

when $x = 0$, $z^* = 0$ and $\dfrac{dz^*}{d\sqrt{x}} = \sqrt{\dfrac{2\rho^*}{c}}$

$x = 1$, $z^* = 0$ and $\dfrac{dz^*}{dx} = 0$

i.e., z^* is the thickness distribution of an aerofoil section, cusped at the trailing edge, with leading edge radius ρ^* . In practice it may be convenient to assume that $\rho^* = \rho$, i.e., that the leading edge radius is not significantly altered by the presence of the boundary layer. Hence the function $S^{(1)}(x)$ evaluated for the displacement surface becomes

$$S^{(1)}(x) = \frac{1}{\pi}\int_0^1 \frac{dx^*}{dy}\frac{dy}{x-y} + \frac{d^*}{\pi}\int_0^1 \frac{dF}{dy}\frac{dy}{x-y} - \frac{\sigma}{\pi}\int_0^1 \frac{dG}{dy}\frac{dy}{x-y}$$

$$+ \frac{\sigma}{\pi}\int_1^{1+X} \frac{dy}{x-y} + \frac{2P}{\pi}\int_1^{1+X} \frac{y-1}{x-y}\,dy + \frac{3Q}{\pi}\int_1^{1+X} \frac{(y-1)^2}{x-y}\,dy$$

$$\ldots (17)$$

with similar expressions for $S^{(2)}(x)$ and $S^{(3)}(x)$. The first integral, involving z^*, can be evaluated by the Weber method (Ref. 4) and the other integrals evaluated analytically taking Cauchy principal values throughout. Thus $S^{(1)}(x)$ can be written concisely as

$$S^{(1)}(x) = S^{(1)*}(x) + d^*\phi_1(x) + \sigma\phi_2(x) + P\phi_3(x) + Q\phi_4(x) \quad \ldots (18)$$

where $S^{(1)*}(x) = \sum_{\mu=1}^{N-1} s_{\mu\nu}^{(1)} z_\mu^*$

Similarly the functions $S^{(2)}(x)$ and $S^{(3)}(x)$ can be written

$$S^{(2)}(x) = S^{(2)*}(x) + d^*\chi_1(x) + \sigma\chi_2(x) \quad \ldots (19)$$

$$S^{(3)}(x) = S^{(3)*}(x) + d^*\psi_1(x) + \sigma\psi_2(x) + P\psi_3(x) + Q\psi_4(x) + (d^* - C_D/4)\psi_5 \quad \ldots (20)$$

The functions $\phi_1 \ldots \phi_4$; χ_1 , χ_2 ; $\psi_1 \ldots \psi_5$ are listed in Appendix 1, and the influence coefficients $s_{\mu\nu}^{(n)}$, n=1,2,3, are tabulated in Ref. 4.

Thus, given the aerofoil geometry and the boundary layer displacement thickness distributions on both surfaces of the aerofoil, the constants d^* , σ and α^* can be evaluated. The residual thickness distribution can be calculated using equation (16) and the functions $S^{(n)}(x)$, n=1 ... 5 can be evaluated from equations (14), (15), (18), (19) and (20), and the pressure distribution from equation (9).

3.2 Calculation of trailing edge pressure

At the trailing edge of the aerofoil the pressure coefficient, which is equal on the upper and lower surfaces, is given by

$$(C_p)_{TE} = 1 - \frac{\cos^2\alpha^* [1 + S^{(1)}(1)]^2}{1 + \sigma^2} \quad \ldots (21)$$

where

$$S^{(1)}(1) = S^{(1)*}(1) + d^*\phi_1(1) + \sigma\phi_2(1) + P\phi_3(1) + Q\phi_4(1)$$

From equations (15) .... (18) of Appendix 1, evaluated for the trailing edge, i.e., x = 1 ,

$$\phi_1(1) = \frac{3}{\pi} \qquad \phi_2(1) = \frac{1}{\pi}(-2.5 - \log X)$$

$$\phi_3(1) = \frac{2}{\pi}(-X) \qquad \phi_4(1) = \frac{3}{\pi}(-\tfrac{1}{2}X^2)$$

and/

and from Ref. 4 ,

$$S^{(1)*}(1) = \sum_{\mu=1}^{N-1} \frac{(-1)^{\mu} - 1}{N} \cdot \frac{2 \sin \theta_{\mu}}{(1 - \cos \theta_{\mu})^2} \cdot z^{*}_{\mu} \; ; \quad \theta_{\mu} = \frac{\mu\pi}{N} \qquad \ldots (22)$$

Using the expressions for P and Q from equation (13), the function S(1) becomes

$$S^{(1)}(1) = S^{(1)*}(1) + \frac{1}{\pi}\left[3d^{*} \frac{1 + X}{X} - \sigma \log X - \frac{3C_D}{4X} \right] \qquad \ldots (23)$$

and using equations (21), (22) and (23) the trailing edge pressure can be evaluated.

Equation (22) is sensitive to small changes in the thickness ordinates of the residual aerofoil close to the trailing edge. The values of these ordinates will not be known with a high degree of accuracy since this would imply an unreasonably good knowledge of the precise behaviour of the boundary layer close to the trailing edge. Therefore it is recommended that equation (22) be used only with a small value of N , the number of reference stations along the chord. A value of N = 8 seems adequate for this purpose.

4. Compressibility Corrections

The hypothesis has been made that the flow about an aerofoil with a boundary layer can be represented by the inviscid flow about a suitably chosen displacement surface. In the absence of any evidence to the contrary, it will be assumed that this hypothesis is equally valid in the case of compressible subsonic flow, provided of course that the boundary layer displacement thickness appropriate to the particular Mach number is used to define the displacement surface. The equation for the velocity distribution (equation 9) can therefore be generalised to deal with compressible flow in the following manner

$$\left(\frac{V}{V_0}\right)^2 = \frac{\left[\cos \alpha^{*} \cdot \left(1 + \frac{S^{(1)}}{B} \pm \frac{S^{(4)}}{\beta}\right) \pm \frac{\sin \alpha^{*}}{\beta}\left(1 + \frac{S^{(3)}}{B}\right)\sqrt{\frac{1 - x}{x}}\right]^2}{1 + \left[\frac{S^{(2)} \pm S^{(5)}}{B}\right]^2} \qquad \ldots (24)$$

where B and β are compressibility factors applied to the contributions to the velocity distribution due to thickness and camber respectively. The precise form that these factors should take is discussed in Refs. 6 and 7, which recommend the following

$$\beta = (1 - M_0^2)^{\frac{1}{2}} \qquad \ldots (25)$$

$$B = (1 - M_0^2(1 - C_{p_i}))^{\frac{1}{2}} \qquad \text{Ref. 6.} \qquad \ldots (26a)$$

or

$$B = (1 - M_0^2(1 - M_0 C_{p_i}))^{\frac{1}{2}} \qquad \text{Ref. 7.} \qquad \ldots (26b)$$

where/

where

$$C_{P_i} = 1 - \frac{(1 + S^{(1)})^2}{1 + (S^{(2)})^2} .$$

The pressure coefficient C_p is calculated from the compressible form of Bernoulli's equation which, taking the value $\gamma = 1.4$ for air, becomes

$$C_p = \frac{1}{0.7\, M_0^2} \left[\left\{ 1 + 0.2\, M_0^2 \left[1 - \left(\frac{V}{V_0} \right)^2 \right] \right\}^{3.5} - 1 \right] \quad \ldots (27)$$

It should be noted that the compressibility factors appearing above are of two kinds. The first, B (equation 26a or 26b) applies only to the thickness terms; and for the reasons given at the beginning of the introduction and illustrated in Fig. 1, it is reasonable to justify this factor by reference to experimental results for symmetrical aerofoils at zero incidence, as well as to higher order theories. This has been done in considerable detail in Ref. 7, and as a result the modified factor (26b) is definitely to be preferred. The situation with regard to the lifting terms, and in particular the justification for using the simple Prandtl-Glauert factor β in them, is however much less satisfactory; and a re-appraisal of the subject is desirable now that a method exists for predicting the viscous pressure distribution, so that a more valid comparison between theory and experiment would now be possible.

5. Comparison between Computed and Experimental Results

In order to assess the accuracy of the method described in this report it is necessary to make use of tests on aerofoils in which not only the pressure distribution was measured, but also the boundary layer displacement thickness, thus eliminating any sources of error in predicting the boundary layer. Such tests are rare. Comparison has been made in the case of the RAE 101 aerofoil, tested at a Reynolds number of 1.6×10^6, at incidences of 4.09° and 8.18° (Ref. 8). The boundary layer displacement thickness was measured at 7 stations on the chord on each surface, and an interpolated displacement thickness distribution based on these measurements was used in the calculation. Figs. 4 and 5 show a comparison between the measured and predicted pressure distributions at the two incidences. Good agreement is achieved in both cases, the lift coefficient being overestimated by approximately 3%.

In the introduction mention was made of the calculation of the pressure distribution on an aerofoil ab initio using an iterative process involving the present method and a theoretically predicted boundary layer. Three such calculations have been made to explore the feasibility of the process. In each case the boundary layer characteristics were calculated by the method of Nash and Macdonald (Ref. 9). To check the accuracy of the predicted boundary layer the combined method was first used to predict the pressure distribution and boundary layer displacement thickness on the RAE 101 aerofoil section referred to above for which measured boundary layer data was available. Fig. 6 shows a comparison between the measured and predicted displacement thickness on the two aerofoil surfaces for incidences of 4.09° and 8.18°. The quoted transition positions (Ref. 8) were used in the calculations and are shown in the figures.

The pressure distributions calculated using the theoretically predicted boundary layer data are almost identical with those calculated using measured data and shown in Figs. 4 and 5, the mean difference in the pressure coefficient C_p being approximately 0.005. The comparison indicates that for typical aerofoil pressure distributions the method of Ref. 9 should be adequate for use in conjunction with the method of this report to calculate the pressure distributions on aerofoils. Fig. 7 shows a comparison between the measured and predicted pressure distributions on a 14% thick cambered aerofoil, designed to carry lift over the rear part of the chord, and tested at a Reynolds number of 1.16×10^6 at an incidence of 3.2°. The calculation was carried out as described above using observed transition positions on the aerofoil surfaces. Again, the agreement is good over the majority of the chord.

These three calculations indicate the possibility of predicting, with reasonable accuracy, the pressure distribution on an aerofoil in viscous flow almost entirely theoretically using the present method and a method such as that described in Ref. 9 for predicting the boundary layer characteristics.

6. Concluding Remarks

A theory and a numerical technique have been developed for predicting the pressure distribution on a thick cambered aerofoil at incidence when the boundary layer displacement thickness is known. This method shows good agreement with the limited experimental data available. The absence of suitable experimental results at high Reynolds numbers and high subsonic Mach numbers makes it impossible to thoroughly assess the accuracy of the method, in particular the compressibility corrections discussed in Section 4. In the case of predicting results at high Reynolds number, the fact that the results must lie between inviscid theory (infinite Reynolds number) and results such as those presented here suggest that the method should be at least as accurate in those cases. It is hoped that tests to be made in the near future at Mach numbers up to $M = 0.7$ including the measurement of the boundary layer characteristics will rectify this omission.

At present no satisfactory method exists which will predict transition position. Until such a method is found, the transition positions on the upper and lower surfaces of the aerofoil must be specified independently of the boundary layer calculation. This has been done in all the calculations referred to in this report.

Comparisons between theory and experiment have been presented for the RAE 101 aerofoil and a cambered aerofoil for which the boundary layer data were obtained theoretically using observed transition positions. These comparisons indicate that methods now exist for calculating turbulent boundary layer data with sufficient accuracy which, when used in conjunction with the theory developed in this report, enables the pressure distribution on an aerofoil in viscous flow to be predicted almost entirely theoretically. This is being investigated in greater detail and will form the basis of a separate report.

Acknowledgment

The author is indebted to the Superintendent, Aerodynamics Division, NPL, for the opportunity to carry out this work; and to Mr. H. H. Pearcey and Dr. R. C. Lock, also of the Aerodynamics Division, for their encouragement and helpful criticism.

References/

References

No.	Author(s)	Title, etc.
1	J. H. Preston	The calculation of lift taking account of the boundary layer. A.R.C. R. & M.2725, 1949.
2	D. A. Spence and J. A. Beasley	The calculation of lift slopes, allowing for boundary layer, with applications to the RAE 101 and 104 aerofoils. A.R.C. R. & M.3137, 1958.
3	J. F. Nash	Turbulent boundary layer behaviour and the auxiliary equation. A.R.C. C.P.835, 1965.
4	J. Weber	The calculation of the pressure distribution on the surface of two-dimensional and swept wings with symmetrical aerofoil sections. A.R.C. R. & M.2918, 1953.
5	J. Weber	The calculation of the pressure distribution on the surface of thick cambered wings, and the design of wings with given pressure distributions. A.R.C. R. & M.3026, 1955.
6	J. A. Bagley	Some aerodynamic principles for the design of swept wings. Prog. in Aeronaut. Sciences, Vol. 3, p.1., Pergamon Press, 1962.
7	P. G. Wilby	The calculation of sub-critical pressure distributions on symmetrical aerofoils at zero incidence. A.R.C. C.P.993, 1967.
8	G. G. Brebner and J. A. Bagley	Pressure and boundary layer measurements on a two-dimensional wing at low speed. A.R.C. R. & M.2886, 1952.
9	J. F. Nash and A. G. J. Macdonald	The calculation of momentum thickness in a turbulent boundary layer at Mach numbers up to unity. A.R.C. C.P.963, 1966.
10		NPL Wind-tunnel data (unpublished).

Appendix 1

Functions Used in the Evaluation of $S^{(1)}(x)$, $S^{(2)}(x)$ and $S^{(3)}(x)$

The functions $S^{(n)}(x)$, n=1,2,3, have been defined as

$$S^{(1)}(x) = \frac{1}{\pi} \int_0^{\infty} \frac{dZ_t}{dy} \frac{dy}{x - y} \qquad \ldots (1)$$

$$S^{(2)}(x) = \frac{dZ_t}{dx} \qquad \ldots (2)$$

$$S^{(3)}(x) = \frac{1}{\pi} \int_0^{\infty} \left[\frac{dZ_t}{dy} - \frac{Z_t}{2y(1-y)} \right] \frac{dy}{x - y}$$

$$= S^{(1)}(x) - \frac{1}{2\pi} \int_0^{\infty} \frac{Z_t}{y(1-y)} \frac{dy}{x - y} \qquad \ldots (3)$$

where Z_t is defined in equation (2).

It is shown in Section 3.1 that $S^{(1)}(x)$, $S^{(2)}(x)$ and $S^{(3)}(x)$ can be expressed in terms of the functions $\phi_1(x) \ldots \phi_4(x)$; $\chi_1(x)$, $\chi_2(x)$; $\psi_1(x) \ldots \psi_5(x)$. These functions are tabulated below, both in their integral form and functional form.

$$\phi_1(x) = \frac{6}{\pi} \int_0^1 \frac{y(1-y)dy}{x-y} \qquad \ldots (4)$$

$$\phi_2(x) = \frac{1}{\pi} \left[\int_0^1 \frac{y(3y-2)dy}{x-y} + \int_1^{1+X} \frac{dy}{x - y} \right] \qquad \ldots (5)$$

$$\phi_3(x) = \frac{2}{\pi} \int_1^{1+X} \frac{(y-1)dy}{x-y} \qquad \ldots (6)$$

$$\phi_4(x) = \frac{3}{\pi} \int_1^{1+X} \frac{(y-1)^2 dy}{x-y} \qquad \ldots (7)$$

$$\chi_1(x) = 6x(1 - x) \qquad \ldots (8)$$

$$\chi_2(x) = x(3x - 2) \qquad \ldots (9)$$

$\psi_1(x)$/

$$\psi_1(x) = \phi_1(x) - \frac{1}{2\pi}\left[\int_0^1 \frac{y(3-2y)\,dy}{(1-y)(x-y)} + \int_1^\infty \frac{dy}{y(1-y)(x-y)}\right] \quad \ldots (10)$$

$$\psi_2(x) = \phi_2(x) - \frac{1}{2\pi}\left[-\int_0^1 \frac{y\,dy}{x-y} - \int_1^{1+X} \frac{dy}{y(x-y)}\right] \quad \ldots (11)$$

$$\psi_3(x) = \phi_3(x) - \frac{1}{2\pi}\left[-\int_1^{1+X} \frac{(y-1)dy}{y(x-y)}\right] \quad \ldots (12)$$

$$\psi_4(x) = \phi_4(x) - \frac{1}{2\pi}\left[-\int_1^{1+X} \frac{(y-1)^2\,dy}{y(x-y)}\right] \quad \ldots (13)$$

$$\psi_5(x) = \frac{1}{2\pi}\int_{1+x}^{\infty} \frac{dy}{y(1-y)(x-y)} \quad \ldots (14)$$

Taking Cauchy principal values of the integrals:

$$\phi_1(x) = \frac{6}{\pi}\left[x(1-x)\log\frac{x}{1-x} + x - \tfrac{1}{2}\right] \quad \ldots (15)$$

$$\phi_2(x) = \frac{1}{\pi}\left[x(3-2x)\log x + (3x+1)(1-x)\log(1-x) - \log(1+X-x) - 3x + \tfrac{1}{2}\right] \quad \ldots (16)$$

$$\phi_3(x) = \frac{2}{\pi}\left[(1-x)\log\frac{1+X-x}{1-x} - X\right] \quad \ldots (17)$$

$$\phi_4(x) = -\frac{3}{\pi}\left[(1-x)^2\log\frac{1+X-x}{1-x} + \tfrac{1}{2}X^2 - X(1-x)\right] \quad \ldots (18)$$

$$\psi_1(x) = \phi_1(x) - \frac{1}{2\pi}\left[\frac{x(3-2x)}{1-x}\log x - 2 + \frac{(1-x)(2x+1)}{x}\log(1-x)\right] \quad \ldots (19)$$

$$\psi_2(x) = \phi_2(x) - \frac{1}{2\pi}\left[1 + x\log\frac{1-x}{x} - \frac{1}{x}\log(1+X) + \frac{1}{x}\log\frac{1+X-x}{1-x}\right] \quad \ldots (20)$$

ψ_3 /

$$\psi_3(x) = \phi_3(x) - \frac{1}{2\pi}\left[\frac{1}{x}\log(1+X) - \frac{1-x}{x}\log\frac{1+X-x}{1-x}\right] \quad \ldots (21)$$

$$\psi_4(x) = \phi_4(x) - \frac{1}{2\pi}\left[\frac{(1-x)^2}{x}\log\frac{1+X-x}{1-x} - \frac{1}{x}\log(1+X) + X\right] \quad \ldots\ldots (22)$$

$$\psi_5(x) = \frac{1}{2\pi}\left[\frac{1}{x(1-x)}\log(1+X-x) - \frac{1}{x}\log(1+X) - \frac{1}{1-x}\log X\right] \quad \ldots (23)$$

Appendix 2/

Appendix 2

The Effect of Wake Displacement Thickness on the Trailing Edge Pressure

The choice of model for the wake displacement thickness will affect the pressure distribution over the aerofoil surface: the effect being progressively more significant over the rear part of the aerofoil and greatest at the trailing edge. It is informative to consider the effect on the trailing edge pressure of a range of wake models.

The trailing edge pressure is given by (Section 3.2)

$$(C_p)_{TE} = 1 - \frac{\cos^2 \alpha^* [1 + S^{(1)}(1)]^2}{1 + \sigma^2} \qquad \ldots (1)$$

Since α^* and σ are small, the pressure is given with good approximation by

$$(C_p)_{TE} = -2 S^{(1)}(1) = -\frac{2}{\pi} \int_0^\infty \frac{dZ_t}{dy} \frac{dy}{x - y} \qquad \ldots (2)$$

where

$$Z_t = z^* + d^* F(x) - \sigma G(x) \qquad 0 \leq x \leq 1$$

$$Z_t = \tfrac{1}{2} \delta_w^* \qquad x > 1$$

Using the constraints listed in Section 2.5, the wake thickness distribution can be expressed in the form

$$Z_t = d^* + \sigma E(x) \qquad x > 1 \qquad \ldots (3)$$

where $E(x)$ satisfies the conditions

$$E(1) = 0 \; ; \quad \frac{dE}{dx}(1) = 1 \; ; \quad E(\infty) = -\frac{4d^* - C_D}{4\sigma}$$

and the trailing edge pressure becomes

$$(C_p)_{TE} = -2 \left[S^{(1)*}(1) + \frac{3d^*}{\pi} + \frac{\sigma}{\pi} \left\{ \int_0^1 \frac{y(3y-2)}{1-y} dy + \int_1^\infty \frac{dE}{dy} \frac{dy}{1-y} \right\} \right] \qquad \ldots (4)$$

where Cauchy principal value of the integrals is taken.

Consider/

Consider the following two wake models which represent reasonably extreme cases:

(i) "rapidly convergent wake", in which the displacement thickness decreases linearly to a value of $\frac{1}{2}C_D$ and remains constant thereafter;

(ii) "slowly convergent wake", in which the displacement thickness decreases exponentially to become asymptotic to the value $\frac{1}{2}C_D$ at infinity.

Typical wake displacement thickness distributions for these two cases are shown in Figs. 8a and 8b. The wake model proposed in Section 2.5 lies between these two extreme cases.

Rapidly convergent wake:

in this case the function $E(x)$ is defined as:

$$E(x) = x - 1 \qquad 1 \leqslant x \leqslant 1 + \frac{1}{k}$$

$$E(x) = C_D/4 \qquad x > 1 + \frac{1}{k} \qquad \ldots (5)$$

where $k = \dfrac{-4\sigma}{4d^* - C_D}$

and equation (4) becomes

$$(C_p)_{TE} = -2\left[S^{(1)*}(1) + \frac{3d^*}{\pi} + \frac{\sigma}{\pi}\left\{ \log k - 2.5 \right\} \right] \qquad \ldots (6)$$

Slowly convergent wake:

in this case the function $E(x)$ is defined as:

$$E(x) = \frac{1}{k}\left(1 - e^{-k(x-1)}\right) \qquad x \geqslant 1 \qquad \ldots (7)$$

and equation (4) becomes

$$(C_p)_{TE} = -2\left[S^{(1)*}(1) + \frac{3d^*}{\pi} + \frac{\sigma}{\pi}\left\{ \log k - 2.5 + \int_0^1 \frac{1-e^{-u}}{u}\,du - \int_1^\infty \frac{e^{-u}}{u}\,du \right\} \right] \qquad \ldots (8)$$

Fig. 8c shows the values of trailing edge pressure given by equations (6) and (8) for aerofoil NPL 3111, for which $d^* = 0.0081$, $\sigma = -0.067$, $S^{(1)}(1) = -0.081$

and/

and C_D was taken as 0.01. Also shown are the values of trailing edge pressure for the wake model proposed in Section 2.5, for a range of values of the parameter X. The extreme values of trailing-edge pressure coefficient are 0.145 and 0.170, a range of only 0.025. Fig. 8c shows the relative insensitivity of trailing-edge pressure to the choice of wake model, and provided that a reasonable value of the parameter X is used, the pressure coefficient can be calculated to within a tolerance of $\pm$ 0.01.

In the predicted pressure distributions shown in Figs. 4, 5 and 6, a value $X = 0.2$ was used.

BMG

FIG. 1

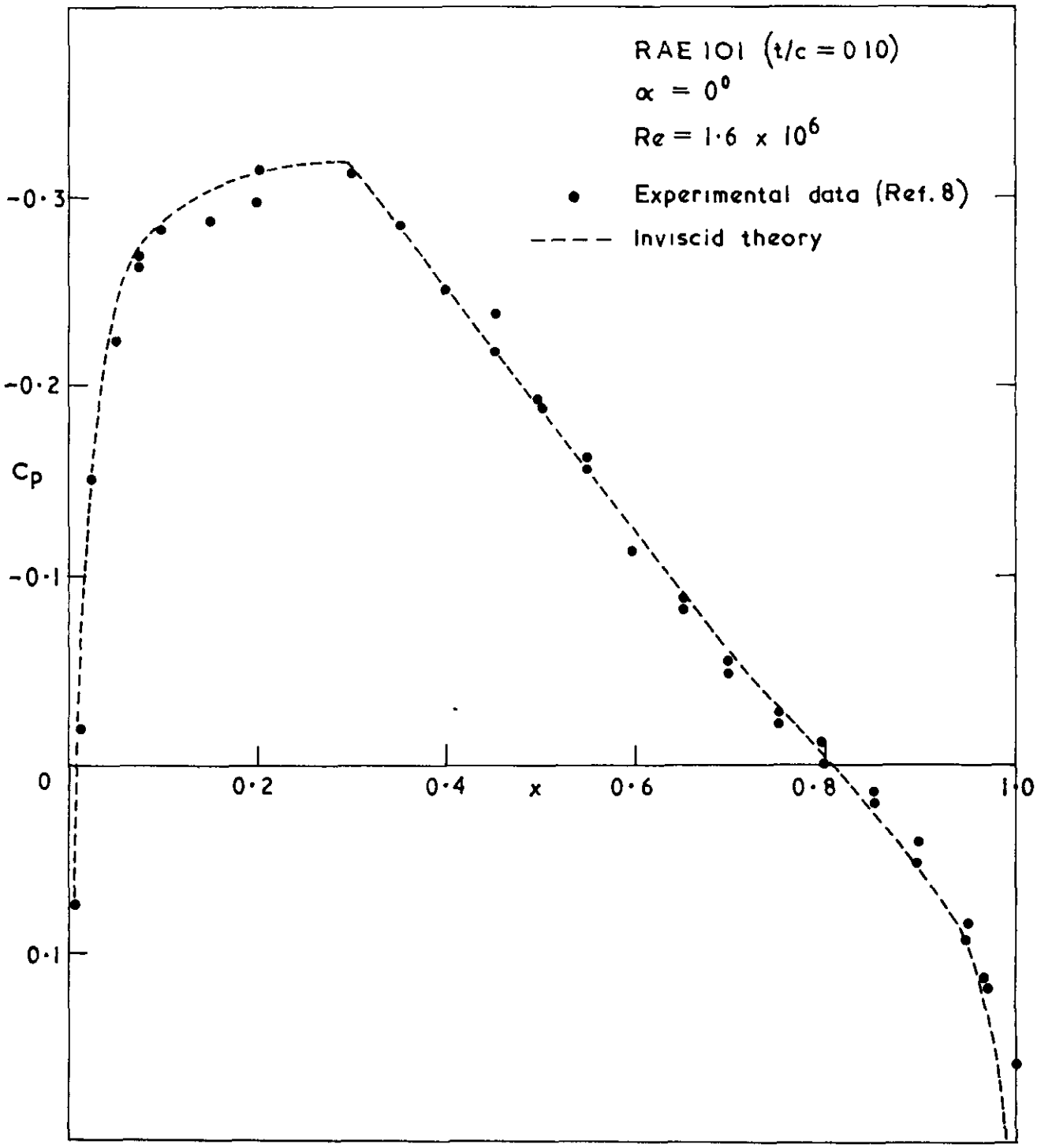

Comparison between experimental pressure distribution and inviscid theory for a symmetric aerofoil at zero incidence

FIG. 2

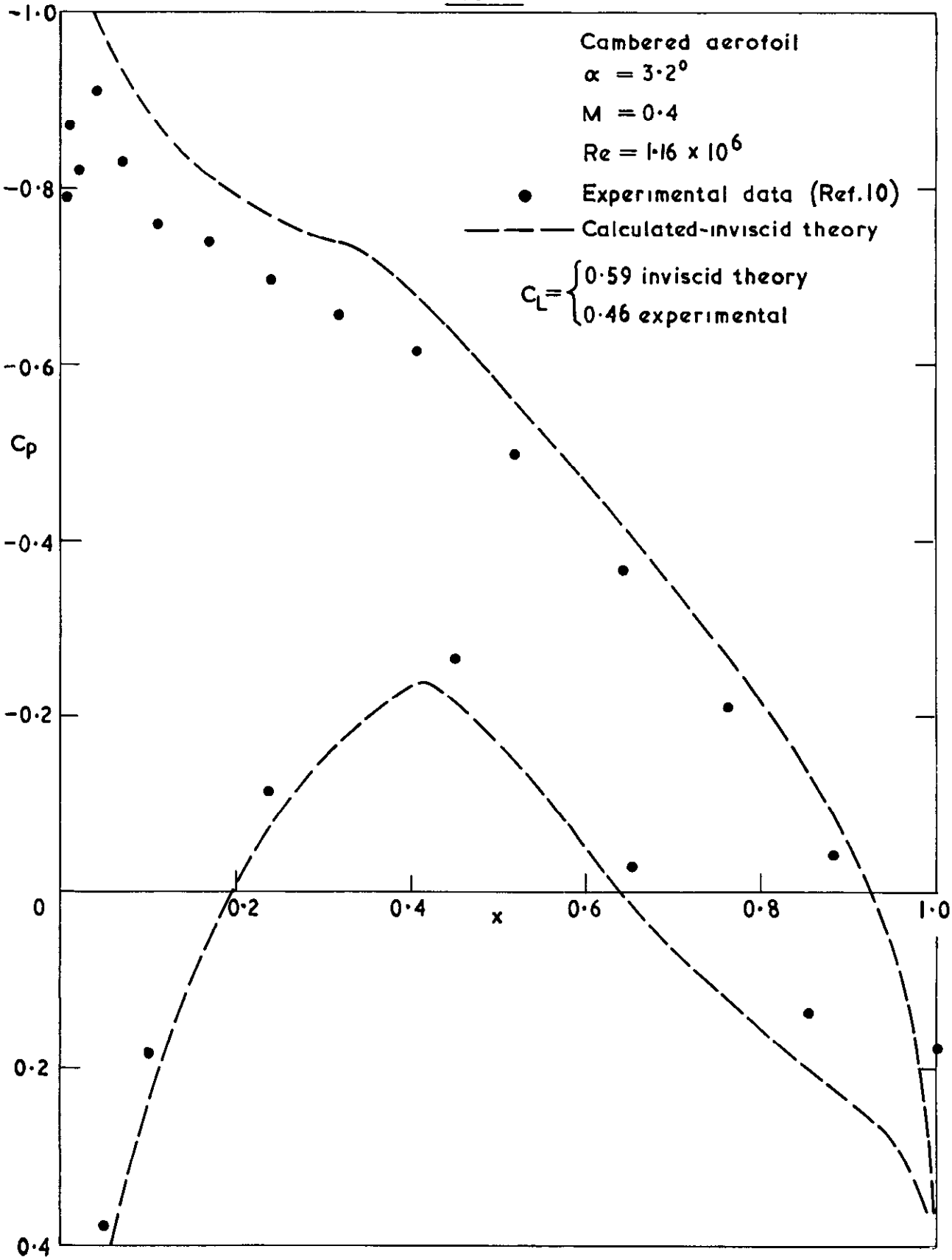

Comparison between experimental pressure distribution and inviscid theory for a cambered aerofoil at incidence

FIGS 3 (a & b)

FIG. 3 (a)

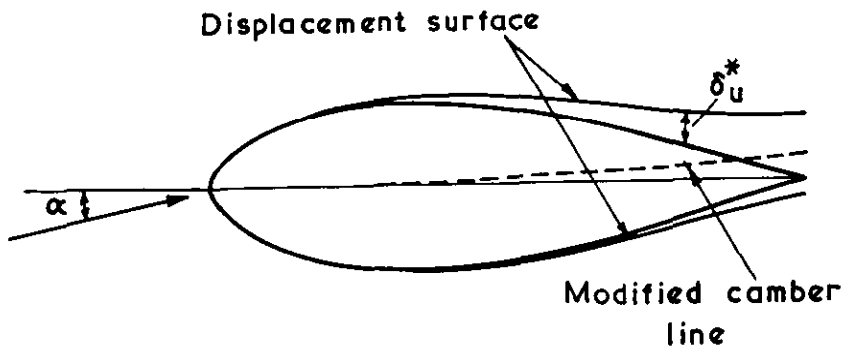

FIG. 3 (b)

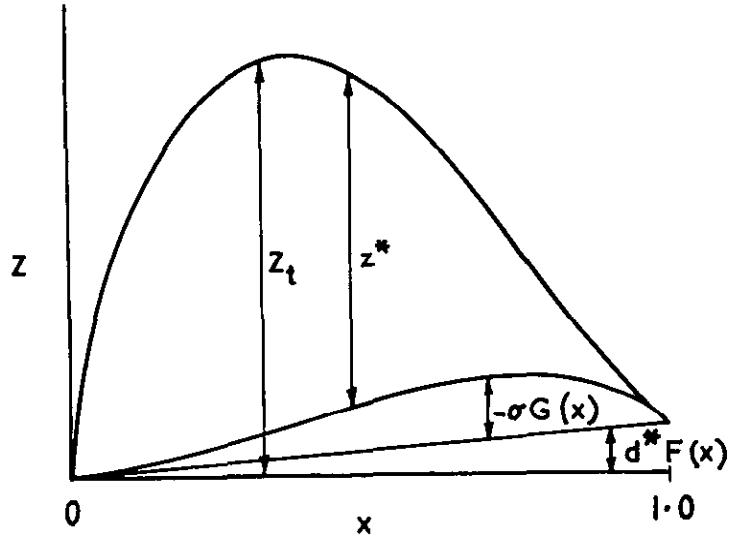

The displacement surface

FIG. 4

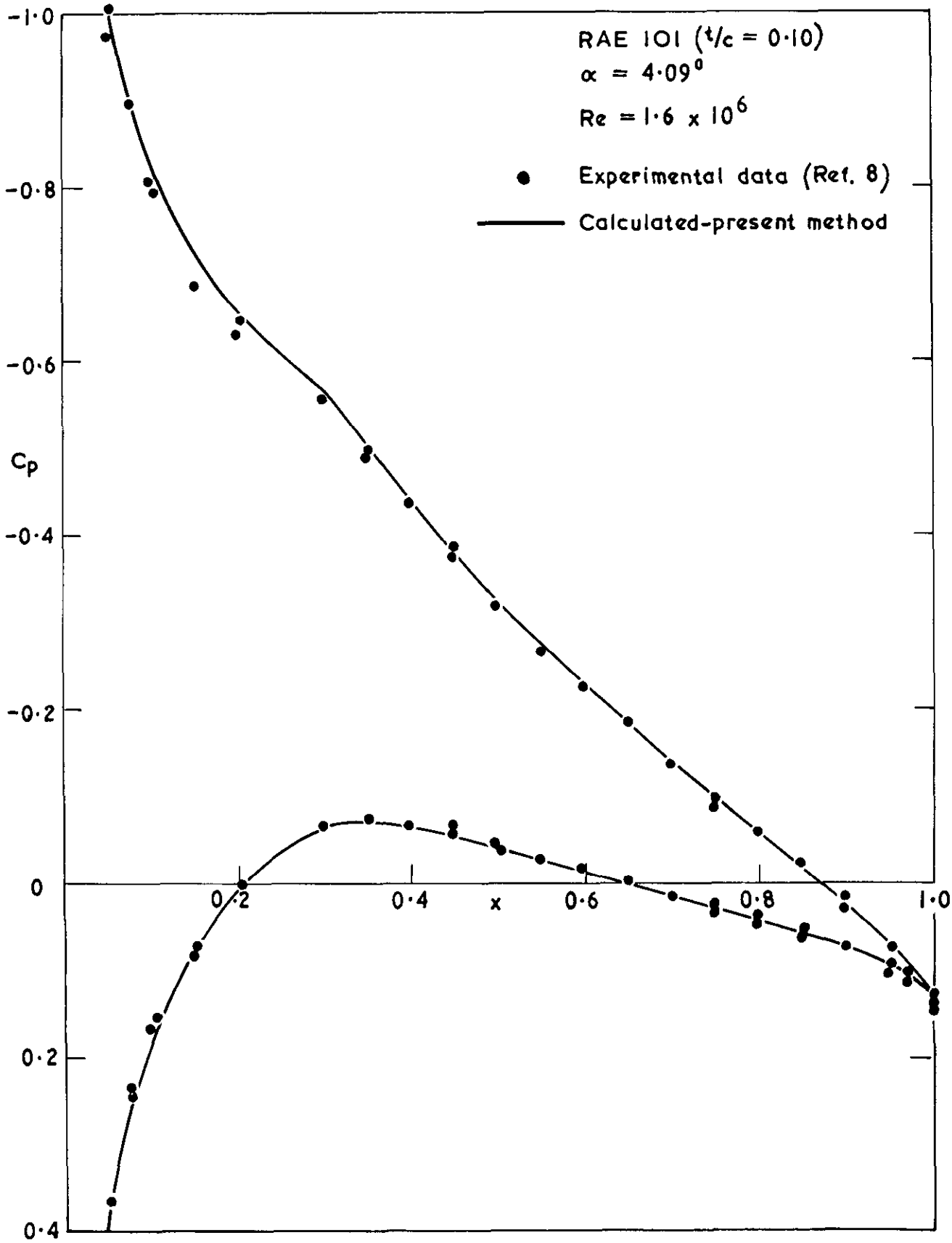

Comparison between predicted and experimental pressure distributions

FIG 5

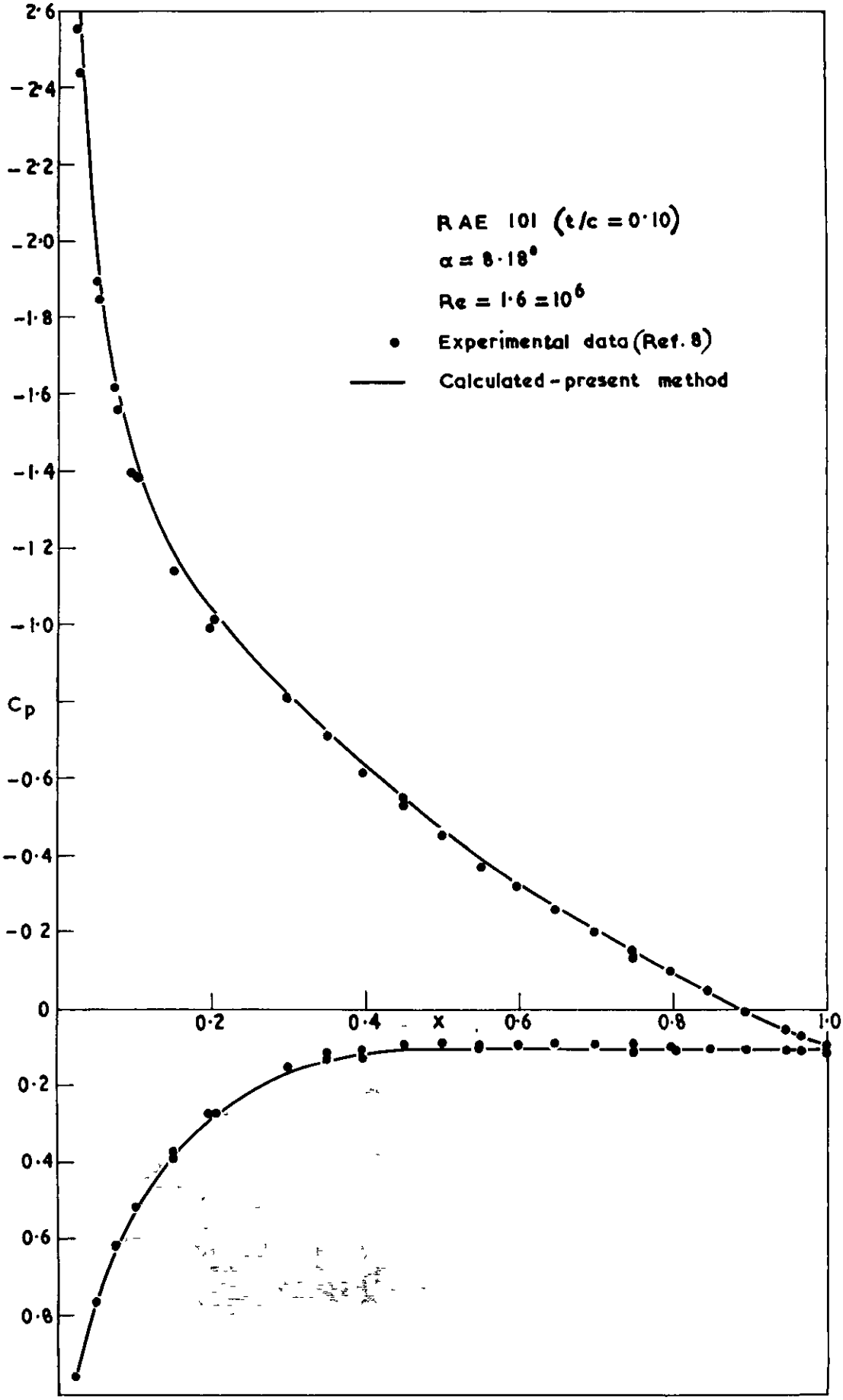

Comparison between predicted and experimental pressure distributions

FIG 6

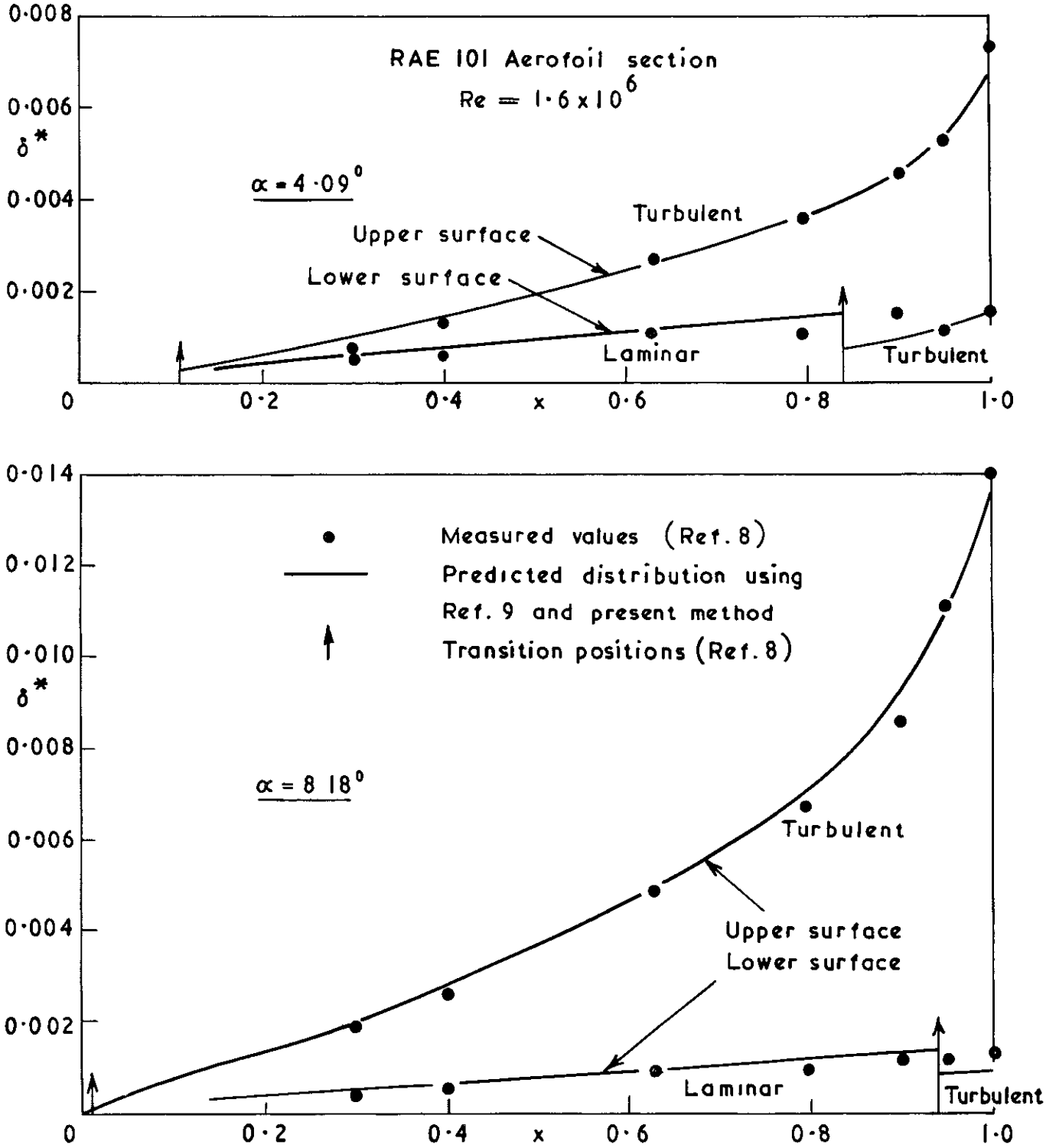

Comparison between measured and predicted boundary layer displacement thickness

FIG. 7

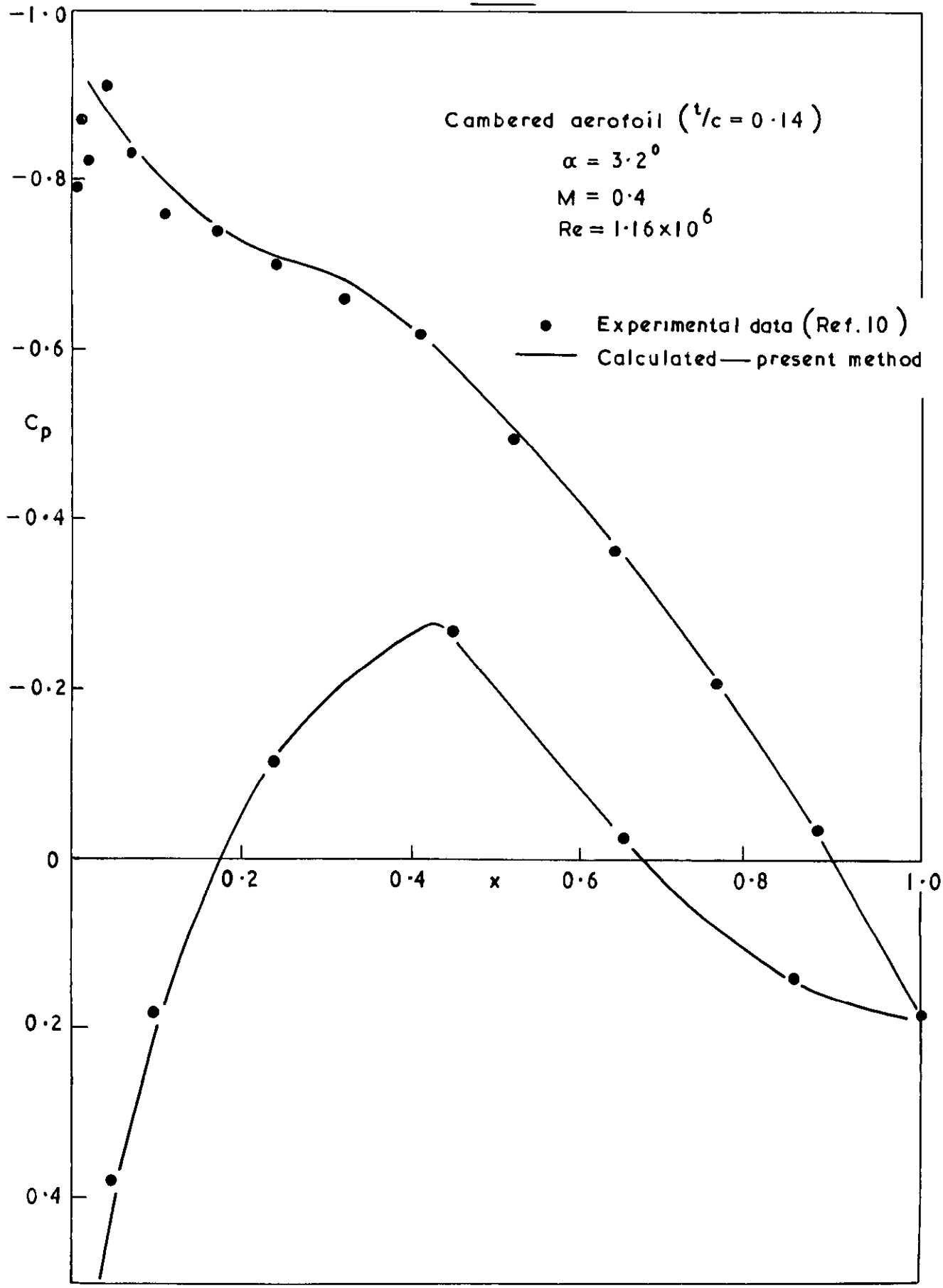

Comparison between predicted and experimental pressure distributions.

FIG.8

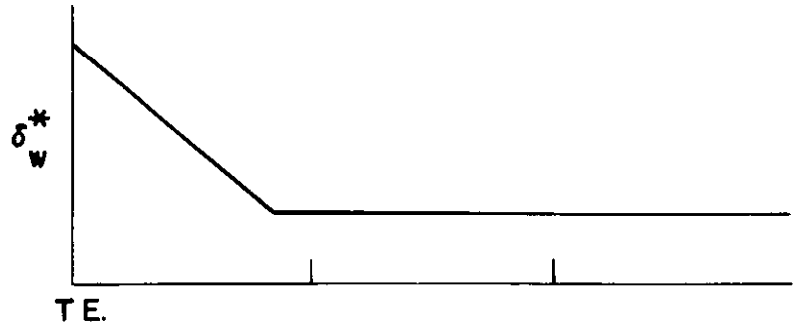

(a) Rapidly convergent wake

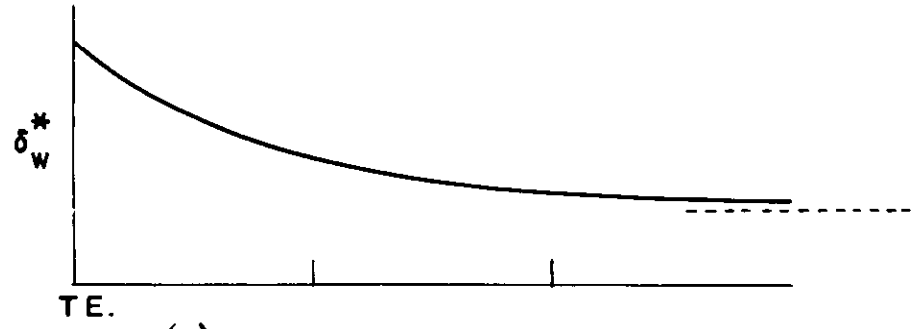

(b) Slowly convergent wake

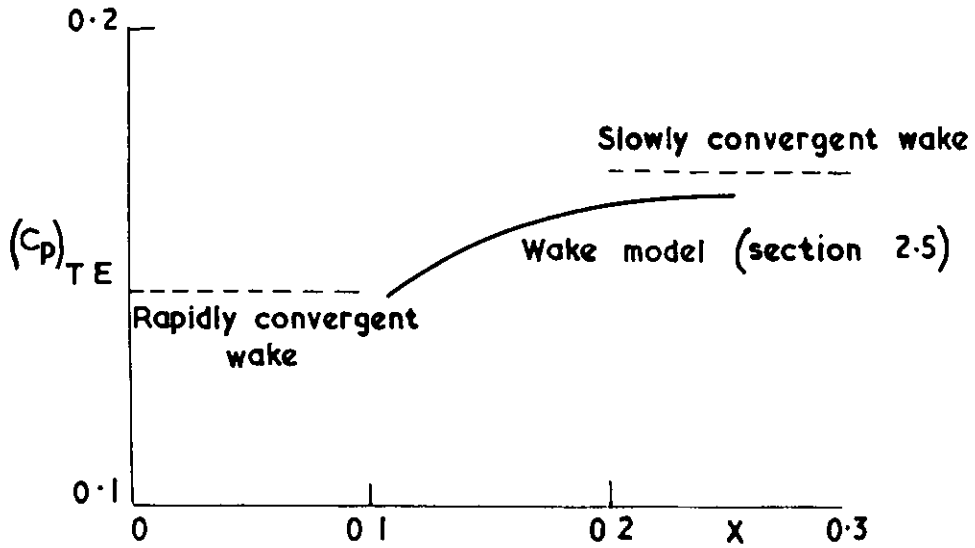

Effect of wake model on T.E. pressure

A.R.C. C.P. No.1005
June, 1967
Powell, B. J.

THE CALCULATION OF THE PRESSURE DISTRIBUTION ON A THICK CAMBERED AEROFOIL AT SUBSONIC SPEEDS INCLUDING THE EFFECTS OF THE BOUNDARY LAYER

A theory and a numerical technique are developed which can be used to predict the pressure distribution on a two-dimensional aerofoil at incidence in a subsonic viscous flow when the boundary layer displacement thickness on the aerofoil surfaces is known.

A few examples are also included of calculated pressure distributions for which the boundary layer data was predicted theoretically.

A.R.C. C.P. No.1005
June, 1967
Powell, B. J.

THE CALCULATION OF THE PRESSURE DISTRIBUTION ON A THICK CAMBERED AEROFOIL AT SUBSONIC SPEEDS INCLUDING THE EFFECTS OF THE BOUNDARY LAYER

A theory and a numerical technique are developed which can be used to predict the pressure distribution on a two-dimensional aerofoil at incidence in a subsonic viscous flow when the boundary layer displacement thickness on the aerofoil surfaces is known.

A few examples are also included of calculated pressure distributions for which the boundary layer data was predicted theoretically.

A.R.C. C.P. No.1005
June, 1967
Powell, B. J.

THE CALCULATION OF THE PRESSURE DISTRIBUTION ON A THICK CAMBERED AEROFOIL AT SUBSONIC SPEEDS INCLUDING THE EFFECTS OF THE BOUNDARY LAYER

A theory and a numerical technique are developed which can be used to predict the pressure distribution on a two-dimensional aerofoil at incidence in a subsonic viscous flow when the boundary layer displacement thickness on the aerofoil surfaces is known.

A few examples are also included of calculated pressure distributions for which the boundary layer data was predicted theoretically.

Printed and published by
HER MAJESTY'S STATIONERY OFFICE

To be purchased from
49 High Holborn, London W C 1
423 Oxford Street, London W 1
13A Castle Street, Edinburgh 2
109 St Mary Street, Cardiff CF1 1JW
Brazennose Street, Manchester 2
50 Fairfax Street, Bristol 1
258–259 Broad Street, Birmingham 1
7–11 Linenhall Street, Belfast BT2 8AY
or through any bookseller

Printed in England

S O. Code No 23-9018-5